Journal of Applied Electrochemistry **34**: 697–704, 2004.
© 2004 *Kluwer Academic Publishers. Printed in the Netherlands.*

Piperidines as corrosion inhibitors for iron in hydrochloric acid

K.F. KHALED[1,†,*] K. BABIĆ-SAMARDŽIJA[2] and N. HACKERMAN[1]
[1]*Department of Chemistry, Rice University, Houston, TX 77005, USA*
[2]*On leave from University of Belgrade, Faculty of Chemistry, Belgrade, Serbia and Montenegro*
Present address: Department of Chemistry, Faculty of Education, Ain Shams University, Roxy, Cairo 11711, Egypt
*(*author for correspondence, fax: +713-348-5155, e-mail: khaled.f@mailcity.com)*

Received 6 April 2003; accepted in revised form 2 October 2004

Key words: corrosion inhibition, hydrochloric acid, iron, piperidines, quantum chemical calculations

Abstract

The objective of this work is to provide additional insight on the influence of substituents on heterocyclic piperidine as acid corrosion inhibitors for iron. This series include piperidine and six derivatives. The inhibiting properties of piperidine and these derivatives were investigated in 1 M HCl by potentiodynamic polarization (dc) and electrochemical impedance spectroscopy measurements, and inhibition was found to increases as 26dp < 35dp < 2mp < 3mp < pip < 4bp < 4mp. Polarization curves suggest that they can all be considered as mixed-type inhibitors. An attempt to correlate electronic properties of the compounds with their experimental efficiencies using molecular orbital calculation methods did not show any clear-cut relationship.

1. Introduction

There is interest in nitrogen-containing organic compounds, such as amines and heterocycles as inhibitors for protecting metallic surfaces from corrosion in various aggressive environments [1–3]. The mode of interaction of the inhibitor molecules with the electrode may be important in understanding the mechanism of inhibition. Inhibitors function by adsorption [2–6] and/or hydrogen bonding to the metal [7, 8]. This in turn depends on the chemical composition and structure of the inhibitor, on the nature of the metal surface, and on the properties of the medium [9, 10]. Structural and electronic parameters, such as the type of functional group, steric and electronic effects, are generally responsible for the inhibition efficiency [11–14]. Relatively high water solubility and low molecular weight of amines is an advantage for their widespread use as corrosion inhibitors [15, 16].

Molecular orbital calculations have been used previously (for example, [10, 13, 17]) to correlate structural and electronic parameters with inhibition efficiencies. Effective correlations would provide an efficient approach to the analysis of the inhibitor–surface interaction.

The aim of this work is to study the influence of piperidines, namely 2-methylpiperidine (2mp), 3-methylpiperidine (3mp), 4-methylpiperidine (4mp), *cis*-2,6-dimethylpiperidine (26dp), 3,5-dimethylpiperidine (35dp) and 4-benzylpiperidine (4bp), on the inhibition of iron corrosion in hydrochloric acid. The dissolution rate was characterized by potentiodynamic polarization (dc) and by electrochemical impedance spectroscopy (EIS). The electronic structure of the amines could be involved in determining interaction with iron surface, therefore correlation between certain molecular orbital calculations and inhibitor efficiencies were sought.

2. Experimental details

Experiments were carried out using pure iron (Puratronic 99.9999% Johnson Mattey), as the electrode material. Iron samples with surface area of 0.28 cm^2 were mounted in Teflon. The surfaces were abraded using emery papers of grit sizes up to 4/0 grit, polished with Al_2O_3 (0.5 μm particle size), cleaned in 18 MΩ water in an ultrasonic bath, and subsequently rinsed in acetone and bi-distilled water.

A conventional electrolytic cell, as described elsewhere [18], was used along with a platinum counter electrode and a saturated calomel reference electrode (SCE). Electrochemical experiments were carried out under static conditions at 25 °C in aerated solutions, using a fine Luggin capillary placed close to the working electrode to minimize ohmic resistance.

The heterocyclic amines studied are presented in Figure 1. All compounds investigated were obtained from Aldrich Chemical Co. They were put in the 1 M HCl (Fisher Scientific) without pretreatment at

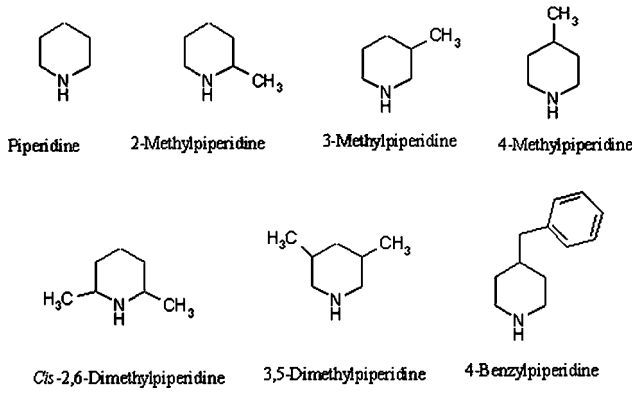

Fig. 1. Chemical structures of investigated heterocyclic amines.

concentrations of 10^{-4}, 10^{-3}, 5×10^{-3}, and 10^{-2} M. The electrode was immersed in these solutions for one hour before starting measurements.

Measurements were performed on an EG&G Princeton Applied Research Potentiostat/Galvanostat (PAR model 273) in combination with a Solarton 1250 frequency response analyzer. The potentiodynamic current-potential curves were obtained by changing the electrode potential by ± 250 mV_{SCE} at a scan rate of 1 m V s^{-1}. EIS measurements were carried out in the frequency range of 100 kHz to 30 mHz with 5 mV peak-to-peak amplitude at open circuit potential. The corrosion software used in this study is model 352-252 version 2.23 and EIS software model 398. Spectra analysis was performed using Zview impedance analysis software (Scribner Associates Inc., Sothern Pines, NC).

Molecular modeling was carried out with Hyperchem version 7, a quantum mechanical program marketed by Hypercube Inc. Molecular orbital (MO) calculations are based on the semi-empirical self-consistent method (SCF) [19, 20]. A full optimization of all geometrical variables (bond lengths, bond angles and dihedral angles) without any symmetry constraint was performed at the restricted Hartree–Fock level (RHF) [21, 22]. We used PM3 [23], AM1 [24], MNDO [25, 26] and MINDO/3 [27] semi-empirical SCF–MO methods in the Hyperchem 7.0 program, implemented on an Intel Pentium 3, 600 MHz computer.

3. Results and discussion

3.1. *Potentiodynamic measurements*

The inhibition efficiency (I) was calculated by applying Equation (1) [18]:

$$I = \left(\frac{i^0_{corr} - i_{corr}}{i^0_{corr}}\right) \times 100 \quad (1)$$

where i^0_{corr} and i_{corr} are uninhibited and inhibited corrosion current densities, respectively.

The anodic and cathodic polarization curves for iron in 1 M HCl, with and without inhibitor, are shown in Figures 2–4. Values of all kinetic parameters such as corrosion potential (E_{corr}), cathodic and anodic Tafel slopes (β_c, β_a) and corrosion current density (i_{corr}) attained by extrapolation of Tafel lines, as well as inhibitor efficiency are listed in Table 1.

The piperidine derivatives decreased i_{corr} significantly for all concentrations studied. The lowest value was obtained for all compounds at 10^{-2} M (Table 1).

The parallel Tafel curves in Figures 2–4, suggest an activation-controlled hydrogen evolution reaction with no change of the proton discharge mechanism. The values of β_c changed with increasing inhibitor concentration, which indicates the influence of the compounds on the kinetics of hydrogen evolution. The shift in the anodic Tafel slope β_a may be due to change in the charge transfer coefficient α_a for the anodic dissolution of iron [6]. This would come about because of an added energy barrier, i.e. the adsorbed inhibitor.

The rapid attainment of corrosion potential in the presence of piperidine and its derivatives suggests that the initial adsorption step involves the piperidinum

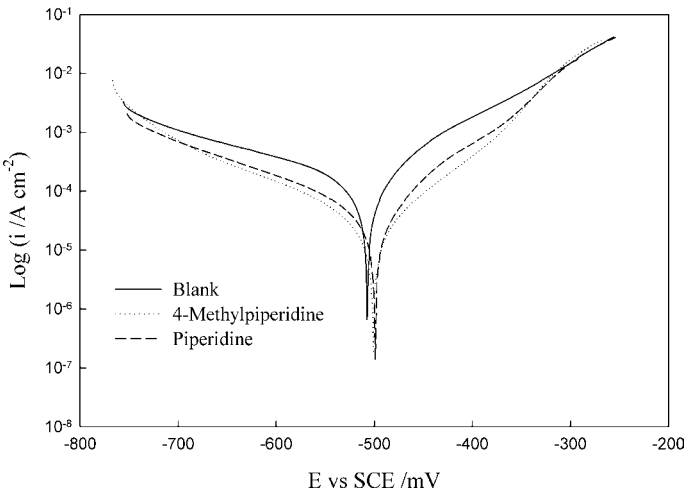

Fig. 2. Anodic and cathodic Tafel lines for iron in uninhibited 1 M HCl and with addition of inhibitors (10^{-2} M).

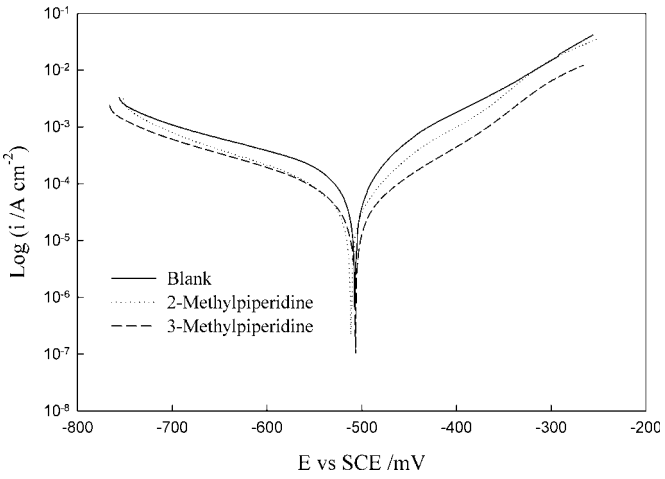

Fig. 3. Anodic and cathodic Tafel lines for iron in uninhibited 1 M HCl and with addition of inhibitors (10^{-2} M).

cations [28]. No definite trend is observed in the shift of corrosion potentials. Thus, these compounds can be classified as mixed-type inhibitors [29].

3.2. *Electrochemical impedance measurements*

A typical set of Nyquist plots for iron in 1 M HCl in the absence and presence of inhibitor is shown in Figure 5. The impedance response of iron changes significantly on inhibitor addition and increases with increasing inhibitor concentration.

The corrosion kinetic values derived from the Nyquist plots and inhibitor efficiency are given in Table 2. Double layer capacitance (C_{dl}), charge transfer resistance (R_{ct}) and inhibitor efficiencies values, were obtained from impedance measurements as described elsewhere [30].

At higher inhibitor concentration, R_{ct} increases and C_{dl} decreases. The latter may result from a reduction in the local dielectric constant and/or from increased electrical double layer thickness. Either of these can be related to adsorption at the metal/solution interface [6].

The addition of heterocyclic amine derivatives provides lower C_{dl} values, probably as a consequence of replacement of water molecules by organic molecules at the electrode surface. Also the inhibitor molecules may reduce the capacitance by increasing the double layer thickness.

3.3. *Spectra analysis*

The impedance analysis (Figure 5) of iron in 1 M HCl shows one depressed capacitive loop (one time constant in the Bode-phase representation).

A Nyquist plot with a depressed semi-circle with the center under the real axis is characteristic for solid electrodes. It is known as frequency dispersion and has been attributed to roughness and other inhomogeneities of the solid surface [31–33]. In these cases the parallel network charge transfer resistance—double layer

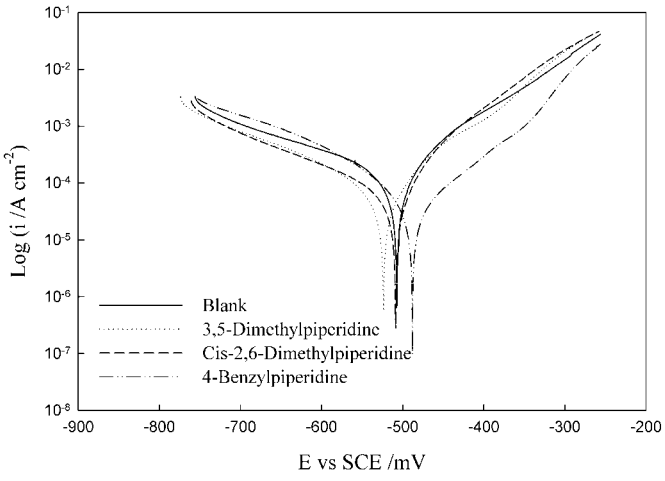

Fig. 4. Anodic and cathodic Tafel lines for iron in uninhibited 1 M HCl and with addition of inhibitors (10^{-2} M).

Table 1. Electrochemical polarization parameters of iron in 1M HCl without and with different concentrations of inhibitors

Compound name	Conc. /M	i_{corr} /μA cm^{-2}	$-E_{corr}$ /mV	β_a /mV dec^{-1}	β_c /MV dec^{-1}	$C{\cdot}R$ /mpy	I /%
Blank		165.4	507.3	92.2	232.1	75.0	–
4MP	10^{-4}	65.17	515.4	87.80	171.8	29.79	60.59
	10^{-3}	53.55	509.5	81.67	166.7	24.48	67.62
	5×10^{-3}	36.29	541.1	82.57	96.46	16.59	78.05
	10^{-2}	20.63	501.1	72.87	124.9	9.43	87.52
4BP	10^{-4}	69.14	518.3	94.56	171.8	31.60	58.19
	10^{-3}	56.54	517.0	94.50	173.2	25.84	65.82
	5×10^{-3}	38.98	488.4	95.67	134.6	17.82	76.43
	10^{-2}	26.77	487.7	100.4	131.1	12.24	83.82
PIP	10^{-4}	73.99	509.3	95.10	163.9	33.82	55.26
	10^{-3}	61.88	512.8	87.71	164.6	28.28	62.58
	5×10^{-3}	45.87	498.0	77.32	166.4	21.00	72.26
	10^{-2}	40.39	499.0	80.36	159.7	18.46	75.58
3MP	10^{-4}	91.52	514.4	105.7	207.0	41.83	44.66
	10^{-3}	68.98	503.4	94.27	162.6	31.53	58.29
	5×10^{-3}	67.20	502.2	92.31	166.0	30.72	59.37
	10^{-2}	48.93	506.5	102.0	171.8	22.36	70.42
2MP	10^{-4}	96.28	515.9	91.46	178.2	44.01	41.78
	10^{-3}	79.89	524.0	92.44	168.2	36.52	51.69
	$5{\cdot}10^{-3}$	76.93	506.0	89.20	200.0	35.16	53.48
	10^{-2}	60.54	511.5	90.12	164.6	27.67	63.39
35DP	10^{-4}	78.79	520.0	94.61	145.8	36.01	52.36
	10^{-3}	77.54	528.3	93.95	179.4	35.44	53.12
	5×10^{-3}	75.60	523.7	94.63	168.8	34.56	54.29
	10^{-2}	74.66	528.4	91.54	167.0	34.13	54.86
26DP	10^{-4}	101.0	499.9	96.29	166.8	46.18	38.93
	10^{-3}	86.13	495.5	91.28	171.9	39.37	47.92
	5×10^{-3}	83.74	508.7	85.66	201.4	38.28	49.37
	10^{-2}	78.06	515.9	90.42	178.3	35.68	52.81

capacitance (R_{ct}–C_{dl}) is usually accepted as a poor approximation [33], especially for systems where an efficient inhibitor is present.

To describe a frequency independent phase shift between an applied AC potential and its current response, a constant phase element (CPE) is generally used [34]. This is defined in the impedance representation as $Z(\omega) = Z_0(j\omega)^{-n}$. Z_0 is the CPE constant, ω is the angular frequency (in rad s^{-1}), $j^2 = -1$, and n is the CPE exponent. Depending on n, CPE can represent resistance ($Z_0 = R$, $n = 0$), capacitance ($Z_0 = C$, $n = 1$), inductance ($Z_0 = L$, $n = -1$) or Warburg impedance for

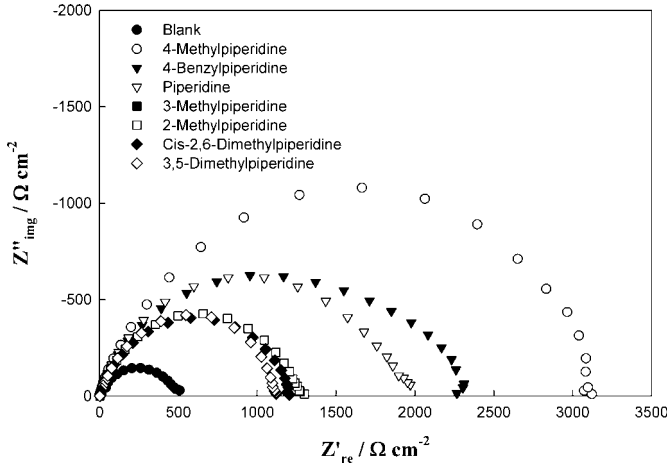

Fig. 5. Nyquist representation of the impedance for iron in 1 M HCl with 10^{-2} M inhibitors.

Table 2. Impedance parameters for the corrosion of iron in 1 M HCl without and with different concentrations of inhibitors

Compound name	Conc. /M	R_{ct} /Ω	10^4 $(1/R_{ct})$ /Ω^{-1}	10^5 C_{dl} /F	I /%	Coverage /θ
Blank		595	16.0	4.23	–	–
4MP	10^{-4}	1303	7.6	1.93	54.31	0.54
	10^{-3}	1504	6.6	1.67	58.42	0.58
	5×10^{-3}	2243	4.4	1.12	73.45	0.73
	10^{-2}	3329	3.0	0.75	82.12	0.82
4BP	10^{-4}	1282	7.8	1.96	53.55	0.53
	10^{-3}	1432	6.7	1.76	59.98	0.59
	5×10^{-3}	1977	5.1	1.27	69.88	0.69
	10^{-2}	2622	3.8	0.96	77.29	0.77
PIP	10^{-4}	1176	8.5	2.14	49.37	0.49
	10^{-3}	1420	7.0	1.77	58.07	0.58
	$5{\cdot}10^{-3}$	1825	5.4	1.38	67.37	0.67
	10^{-2}	2171	4.6	1.16	72.57	0.73
3MP	10^{-4}	948	10.4	2.65	37.19	0.37
	10^{-3}	1205	8.3	2.09	50.58	0.51
	5×10^{-3}	1356	7.3	1.85	56.09	0.56
	10^{-2}	1640	6.1	1.53	63.69	0.63
2MP	10^{-4}	913	10.9	2.75	34.78	0.34
	10^{-3}	1117	8.9	2.25	46.69	0.46
	5×10^{-3}	1198	8.3	2.11	50.30	0.51
	10^{-2}	1406	7.1	1.79	57.65	0.57
35DP	10^{-4}	1123	8.9	2.24	46.98	0.46
	10^{-3}	1175	8.5	2.14	49.33	0.49
	5×10^{-3}	1165	8.5	2.16	48.89	0.48
	10^{-2}	1179	8.4	2.13	49.49	0.49
26DP	10^{-4}	890	11.2	2.83	33.12	0.33
	10^{-3}	1026	9.7	2.45	41.96	0.42
	5×10^{-3}	1064	9.3	2.36	44.04	0.44
	10^{-2}	1292	7.7	1.95	53.91	0.54

($n = 0.5$) [35]. By using the concept of CPE, we had an excellent fit with the experimental data. The equivalent circuit in Figure 6 has been used to model impedance spectra with one capacitive loop [35, 36].

Zview impedance modeling software was used to generate Figure 7 (representative example) for the impedance spectra carried out at the corrosion potential of iron exposed to 1 M HCl without and with the amine derivatives. The simulated and measured results fit very well. Figure 7(a) shows Nyquist plots recorded after 1 h of immersion in 1 M HCl solutions. The diameter of the capacitive loop obtained in HCl solution increases in the presence of piperidine derivatives, an indication of inhibition of the corrosion process.

Bode-phase plots gave only one capacitive time-constant, Figure 7(b). In all cases the high frequency part of the impedance and phase angle describes the behavior of an inhomogeneous surface layer [37]. The low frequency contribution shows the kinetic response for the charge transfer reaction [37].

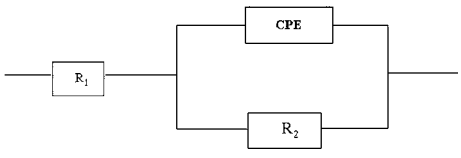

Fig. 6. Equivalent circuit model for the studied inhibitors.

3.4. *Adsorption isotherm*

Adsorbed organic molecules may interact with each other as well as with the electrode surface. The latter may be by chemisorption. In the process water molecules must be displaced from the metal surface [14]. In addition, piperidinum cations [28] can adsorb electrostatically *via* anions already associated with the surface [38].

The degree of surface coverage (θ) for different inhibitor concentrations in 1 M HCl was evaluated from double layer capacitances [30]. These surface coverage values were tested graphically by fitting to a suitable adsorption isotherm. Figure 8 shows that adsorption in this system can be fitted by a Temkin adsorption isotherm [39].

The efficiencies of the methyl-substituted piperidine compounds (Table 1 and 2) can be related to the inductive electronic effect caused by the methyl substituent. Thus, an increase in electronic density on the nitrogen atom should enhance the bond between the nitrogen and iron. The most effective of the compounds in this regard is 4 mp.

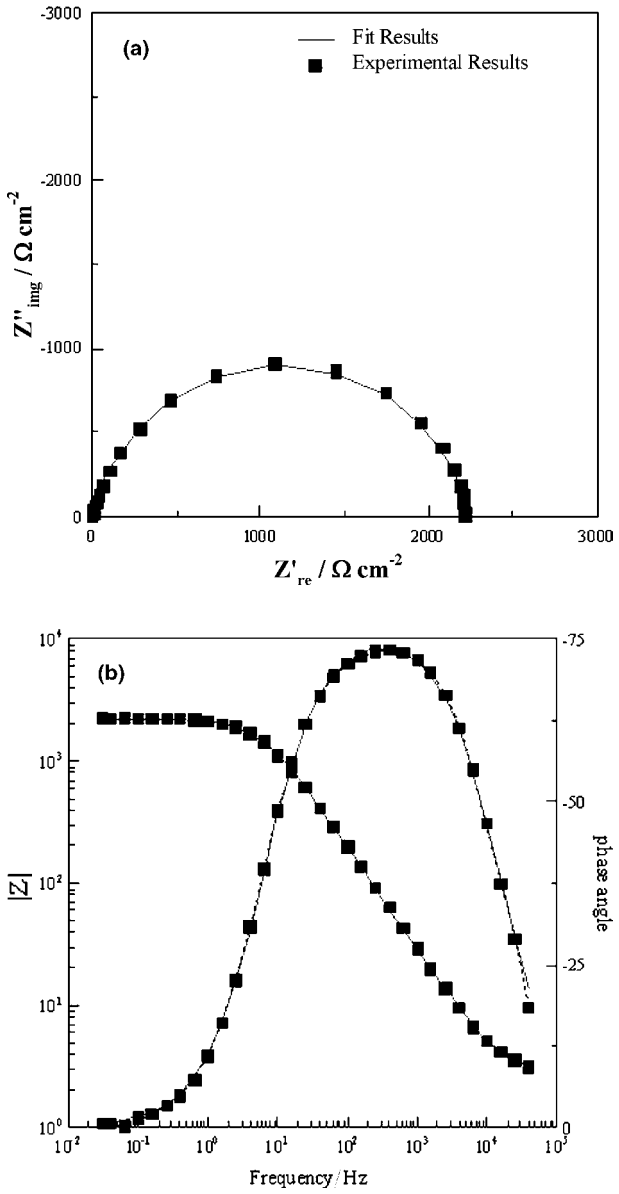

Fig. 7. (a) Nyquist plots of iron in 1 M HCl with 5×10^{-3} M of 4-methylpiperidine at E_{corr}; (b) Bode-phase plots of iron in 1 M HCl solutions with 5×10^{-3} M of 4-methylpiperidine at E_{corr}.

Steric effects may also influence inhibitor efficiency. This would explain the difference between 4- < 3- < 2-methylpiperidine as well as the lower effectiveness of 3,5- < 2,6-dimethylpiperidine.

4-Benzylpiperidine provided good efficiency and high surface coverage due to its additional adsorption center (benzene ring).

3.5. *Molecular theory and experimental corrosion inhibition*

Table 3 contains a number of calculated variables. In addition it has been suggested [10, 17, 40–43], that there should be a relationship between inhibitor efficiency and the difference between the highest occupied molecular orbital (HOMO) and the lowest unoccupied molecular orbital (LUMO).

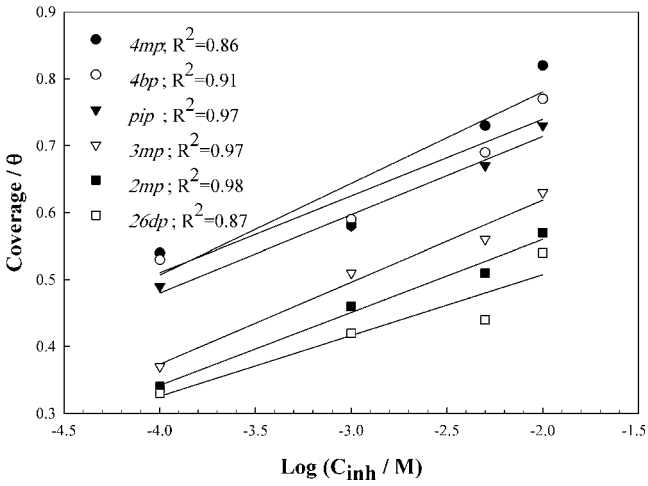

Fig. 8. Temkin adsorption plots of iron in 1 M HCl containing 10^{-2} M of piperidine derivatives.

Figure 9 contains those calculated values for which the correlation coefficients are above 60%. Values not included would reduce the correlation coefficient to an unacceptably low value. Although coefficients of 60% have been considered satisfactory [40], we consider this too low. If we had used all seven compounds the correlation coefficient would have been even lower. The data which are usable show the order of efficiency as 4mp > pip > 3mp > 2mp (Figure 9(a)). In fact the efficiency increases with lower dipole moments, with decreasing molecular size and with increasing nitrogen charge, respectively (Figure 9(b)–(d)). All of these are intuitively hard to accept.

In any event the attempt to relate corrosion inhibitor efficiency to the calculated parameters used here was not sufficient to make a general case. There are a few papers in the corrosion literature in which MO calculations based on molecular structure and corrosion inhibitor structure are said to be related. However, the relation is often based on lower than desirable correlation coefficients or by not using all the data. Based on the literature to date, including this paper, no truly predictive process has yet been identified.

We believe the quantum mechanical approach may well be able to foretell structures that are better for corrosion inhibition purposes. However, the system as treated so far has been oversimplified. For instance, the quantum nature of the surface on which sorption of the inhibitor molecule is to take place is neglected. Are the sorption sites metal atoms or oxide sites or vacancies or kinks? Also, it is necessary to recognize that while the inhibitor molecule must be guided by charge distribution within itself, it is also in sorption competition with other chemical species in the fluid phase.

In summary the value of the approach requires eliminating the implicit assumptions that (i) the effect depends only on the inhibitor molecule properties and (ii) that everything else in its vicinity is uninvolved either with respect to competition for the surface or with respect to itself. Continued efforts to find a theoretical

Table 3. Theoretical calculations obtained using different semi-empirical SCF-MO methods in Hyperchem 7.0 program

Compound name	Method	HOMO /eV	LUMO /eV	HOMO–LUMO gap/eV	μ /D	A^2 grid /Å^2	Q_N /C
4MP	PM3	−9.16	2.85	12.01	1.17	270.3	−0.36
	AMI	−9.28	3.32	12.60	1.15	284.0	−0.30
	MNDO	−9.99	3.05	13.04	1.08	289.9	−0.33
	MINDO/3	−8.61	2.39	11.00	0.21	294.7	−0.20
4BP	PM3	−9.22	0.42	9.64	1.40	385.1	−0.06
	AMI	−9.25	0.56	9.81	1.41	388.2	−0.30
	MNDO	−9.24	0.26	9.50	0.99	395.2	−0.33
	MINDO/3	−8.61	0.96	9.57	0.13	402.9	−0.20
PIP	PM3	−9.16	2.86	12.02	1.19	259.9	−0.06
	AMI	−9.28	3.31	12.59	1.17	258.6	−0.30
	MNDO	−9.99	3.05	13.04	1.08	262.8	−0.33
	MINDO/3	−8.61	1.55	10.16	0.19	266.1	−0.20
3MP	PM3	−9.16	2.84	12.00	1.17	284.5	−0.06
	AMI	−9.28	3.31	12.59	1.17	282.1	−0.30
	MNDO	−9.99	3.04	13.03	1.06	289.8	−0.35
	MINDO/3	−8.62	1.52	10.14	0.19	293.2	−0.19
2MP	PM3	−9.15	2.86	12.01	1.23	278.4	−0.06
	AMI	−9.31	3.31	12.62	1.22	279.0	−0.29
	MNDO	−9.89	2.99	12.88	1.11	284.8	−0.34
	MINDO/3	−8.48	1.49	9.97	0.29	292.8	−0.23
35DP	PM3	−9.12	2.85	11.97	1.10	302.8	−0.58
	AMI	−9.26	3.31	12.57	1.11	304.2	−0.30
	MNDO	−9.99	3.04	13.03	1.02	311.2	−0.33
	MINDO/3	−8.63	1.50	10.13	0.23	315.2	−0.20
26DP	PM3	−9.16	3.42	12.58	1.27	296.9	−0.07
	AMI	−9.29	3.29	12.58	1.25	297.9	−0.29
	MNDO	−9.74	2.92	12.66	1.11	304.7	−0.35
	MINDO/3	−8.61	1.50	10.11	0.35	317.9	−0.22

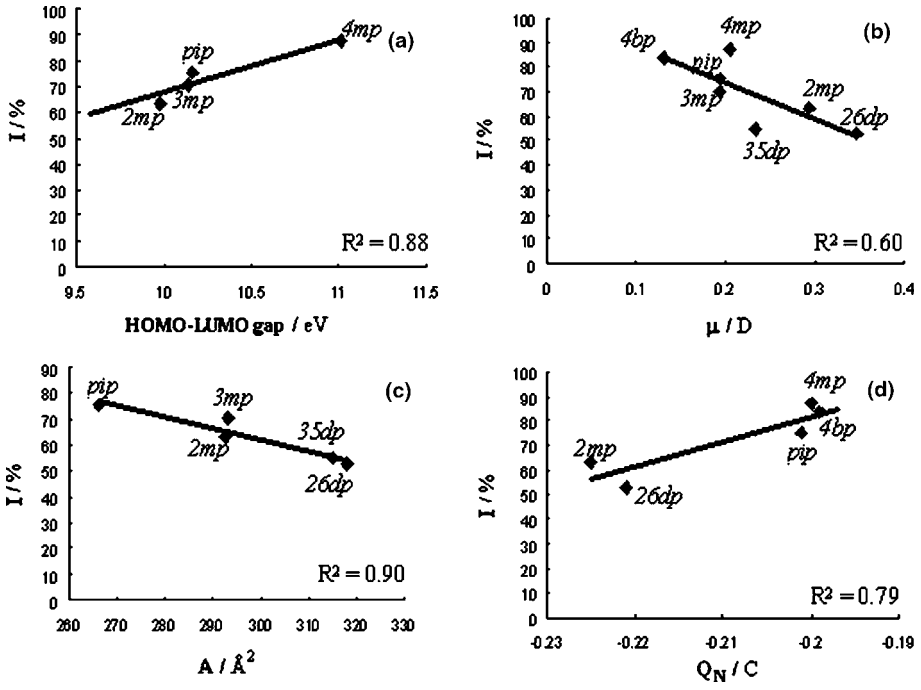

Fig. 9. Graphs of *I*–(HOMO–LUMO gap), μ, *A* and Q_N for piperidine derivatives obtained from MINDO/3, respectively.

basis for predicting corrosion inhibitor efficiencies are required. However, to be of true value, it is imperative that a more substantial theoretical basis must be devised.

4. Conclusions

Potentiodynamic polarization and EIS techniques were used to characterize the corrosion inhibition of iron in 1 M HCl by piperidine and some of its derivatives. All these compounds behave as mixed-type inhibitors. Their adsorption was suitably fitted by Temkin isotherms. The inhibition increased as follows, 26dp < 35dp < 2mp < 3mp < pip < 4bp < 4mp at all inhibitor concentration used.

MO calculations for these compounds give no consistent insight into the reason for the inhibitor efficiency order found. The corrosion literature is replete with relationships between such calculations and inhibitor efficiency, in no case as suggested to predict efficiency from such calculations. This difficulty may stem from the disregard of implicit assumptions regarding the corrosion systems, specifically the competition for adsorption on the interface.

Acknowledgements

The authors' acknowledge the financial support provided by Robert A. Welch Foundation of Houston, Texas, USA.

References

1. P.R. Roberge, 'Handbook of Corrosion Engineering' (McGraw-Hill, 1999).
2. J.M. Sykes, *Br. Corros. J.* **25** (1990) 175.
3. P. Chetterjee, M.K. Banerjee and K.P. Mukherjee, *Indian J. Technol.* **29** (1991) 191.
4. K. Aramaki and N. Hackerman, *J. Electrochem. Soc.* **115** (1968) 1007.
5. K. Aramaki and N. Hackerman, *J. Electrochem. Soc.* **116** (1969) 568.
6. E. McCafferty and N. Hackerman, *J. Electrochem. Soc.* **119** (1972) 146.
7. R.D. Braun, E.E. Lopez and D.P. Vollmer, *Corros. Sci.* **34** (1993) 1251.
8. M.J. Incorvia and S. Contarini, *J. Electrochem. Soc.* **136** (1989) 2493.
9. F. Bentiss, M. Lagrenee, M. Trainsnel and J.C. Hornez, *Corros. Sci.* **41** (1999) 789.
10. J. Cruz, E. Garcia-Ochoa and M. Castro, *J. Electrochem. Soc.* **150** (2003) 26.
11. F. Bentiss, M. Lagrenee and M. Traisnel, *Corrosion* **56** (2000) 733.
12. F. Bentiss, M. Traisnel and M. Lagrenee, *J. Appl. Electrochem.* **31** (2001) 41.
13. Stoyanova, G. Petkova and S.D. Peyerimhoff, *Chem. Phys.* **279** (2002) 1.
14. P. Li, J.Y. Lin, K.L. Tan and J.Y. Lee, *Electrochem. Acta* **42** (1997) 605.
15. R.D. Braun, E.L. Lopez and D.P. Vollmer, *Corros. Sci.* **34** (1993) 1251.
16. T. Szauer and A. Brandt, *Electrochem. Acta* **26** (1981) 1219.
17. V.S. Sastri and J.R. Perumareddi, *Corrosion* **53** (1997) 617.
18. K.F. Khaled, S.S. Abdel-Rehim and N. Hackerman, Proceedings of the 9th European Symposium on Corrosion Inhibitors, Ann. Univ. Ferrara, Vol. 11, 2000, p. 713.
19. C.C.J. Roothaan, *Rev. Mod. Phys.* **23** (1951) 69.
20. W. Thiel, 'Modern Methods and Algorithms of Quantum Chemistry' (NIC Series), 3 (2000) 261.
21. K. Wolinski, J.F. Hinton and P. Pulay, *J. Am. Chem. Soc.* **112** (1990) 8251.
22. M.J.S. Dewar and D.A. Liotard, *J. Mol. Struct.* (*Theochem.*) **206** (1990) 123.
23. J.J.P. Stewart, *J. Comput. Chem.* **10** (1989) 209.
24. M.J.S. Dewar, E. Zoebisch, E.F. Healy and J.J.P. Stewart, *J. Am. Chem. Soc.* **107** (1985) 3902.
25. M.J.S. Dewar and W. Thiel, *J. Am. Chem. Soc.* **99** (1977) 4899.
26. M.J.S. Dewar and W. Thiel, *J. Am. Chem. Soc.* **99** (1977) 4907.
27. R.C. Bingham, M.J.S. Dewar and D.H. Lo, *J. Am. Chem. Soc.* **97** (1975) 1285.
28. S.S. Abdel-Rehim, Magdy A.M. Ibrahim and K.F. Khaled, *J. Appl. Electrochem.* **29** (1999) 593.
29. F. Bentiss, M. Lagrenee, B. Elmehdi, B. Mernari, M. Traisnel and H. Vezin, *Corrosion* **56** (2002) 399.
30. K. Juttner, *Electrochim. Acta* **35** (1990) 1501.
31. T. Pajkossy, *J. Electroanal. Chem.* **364** (1994) 111.
32. W.R. Fawcett, Z. Kovacova, A. Motheo and C. Foss, *J. Electroanal. Chem.* **326** (1992) 91.
33. F. Mansfeld, *Corrosion* **37** (1981) 301.
34. J.R. Macdonald, 'Impedance Spectroscopy—Emphasizing Solid Materials and Systems' (A Wiley-Interscience Publication, 1987).
35. E. McCafferty, *Corros. Sci.* **39** (1997) 243.
36. M.S. Morad, *Corros. Sci.* **42** (2000) 1313.
37. M.S. Abdelaal and M.S. Morad, *Br. Corros. J.* **36** (2001) 253.
38. S. Rengamati, S. Muralidharam, M. Andu Kulandainathan and S. Venkatakrishna Iyer, *J. Appl. Electrochem.* **24** (1994) 355.
39. F.M. Donahue and K. Nobe, *J. Electrochem. Soc.* **114** (1967) 1012.
40. G. Bereket, E. Hur and C. Ogretir, *J. Mol. Struct.* (Theochem.) **578** (2002) 79.
41. I. Lukovits, I. Bako, A. Shaban and E. Kalman, *Electrochim. Acta* **43** (1998) 131.
42. E. Lazarova, S. Kalcheva, G. Neykov, T. Yankova and N. Stoyanov, *J. Appl. Electrochem.* **30** (2000) 561.
43. G. Petkova, E. Sokolova, S. Raicheva and P. Ivanov, *Br. Corros. J.* **31** (1996) 55.